Construction and Building Materials 135 (2017) 580–589

Contents lists available at ScienceDirect

Construction and Building Materials

journal homepage: www.elsevier.com/locate/conbuildmat

Influence of SAP content and curing age on air void distribution of high performance concrete using 3D volume analysis

Babatunde J. Olawuyi [a], William P. Boshoff [b,*]

[a] Department of Building, School of Environmental Technology, Federal University of Technology, P.M.B 64 Minna, Niger-State, Nigeria
[b] Department of Civil Engineering, Stellenbosch University, Private Bag X1, Matieland 7600, Stellenbosch, Western Cape, South Africa

ARTICLE INFO

Article history:
Received 20 July 2016
Received in revised form 31 October 2016
Accepted 21 December 2016

Keywords:
Computed tomography (CT) scanning
3D-void analysis
High-performance concrete
Air void distribution
Superabsorbent Polymers (SAP)
SAP content
Binder type
Curing age

ABSTRACT

Incorporating Superabsorbents Polymers (SAP) as internal curing agents (IC-agents) in high performance concrete (HPC) for mitigation of autogenous shrinkage is one new trend in concrete practice. SAP's water absorption and desorption as cement hydrates however leaves micro voids within the concrete which can negatively influence the mechanical properties of HPC. The SAP content, sizes, binder composition, solid constituents of concrete and curing age could be of direct influence on the resultant air voids sizes and its distribution in concrete. This paper therefore reports on three dimensional (3D) volume analysis of the influence of SAP contents and curing age on air voids distribution in HPC. Four HPC mixtures with different binder constituents and water/binder (W/B): M_{1F} and M_{1S} (0.2), M_2 (0.25) and M_3 (0.3) were tested with two grain sizes of SAP ($SP_1 \leqslant 300$ μm *and* $SP_2 \leqslant 600$ μm). The SAP contents were also varied (0%; 0.2%; 0.3%; and 0.4%) by weight of binder. Concrete cylinders (50 mm Θ × 100 mm) were cast and cured in water for different ages (7, 28, 56 and 90 days) before the hardened HPC was subjected to X-ray computed tomography (CT) scanning for determination of the air void distribution. The analysed 3D X-ray images gave results on SAP grain sizes, SAP air voids, distribution and volume in the HPC with the respective influence of binder type, W/B and curing age assessed.

1. Introduction

High-performance concrete (HPC) is defined by ACI [1] as concrete meeting special combinations of performance and uniformity requirements that cannot always be achieved routinely using conventional constituents and normal mixing, placing, and curing practice. HPCs are typically of low water/binder (W/B) with very dense microstructures even at early age which hinders the possibility of sufficient rapid transportation of curing water into the interior especially in concrete with large dimensions. Hence the need for internal curing (IC) in HPC through the use of high water storing materials as admixtures for supply of water to the surrounding matrix soon as self-desiccation begins [2–4].

Research efforts at mitigating autogenous-shrinkage-caused-cracking to which HPC and ultra-high performance concrete (UHPC) are susceptible, has resulted in IC approaches adopting saturated lightweight aggregates (LWA) and Superabsorbent Polymers (SAP) as IC-agents [5–7]. The use of SAP as IC-agent has been adjudged to be effective for the mitigation of autogenous shrinkage in concrete especially HPC via its absorption and desorption of water internally as the cement hydrates [7]. It however leaves micro voids which can negatively influence the mechanical properties of the concrete.

The main driving force for the swelling of SAP as reported in the RILEM State-of-the-Art Reports (STAR) Volume 2 by the TC 225 [7] is the osmotic pressure which is proportional to the concentration of ions in the aqueous solution. As the ions in SAP are forced closely together by the polymer network, there exists a very high osmotic pressure within. By absorption of water, the osmotic pressure is reduced by diluting the charges (Fig. 1). The reset force of the polymer network and the external osmotic pressure thus work together to offset the osmotic driving force. Other external pressure such as from the swelling of SAP or retention of water against external mechanical forces reduces the absorption capacity of the SAP. The swelling is thereby in equilibrium when all forces are equal [7–9].

The absorption of a SAP is argued by Mechtcherine & Reinhardt [7] to be strictly dependent on the concentration of ions in the swelling medium which can be influenced by the binder composition and microstructure. Kinetics of water migration in

* Corresponding author.
E-mail addresses: babatunde@futminna.edu.ng (B.J. Olawuyi), bboshoff@sun.ac.za (W.P. Boshoff).

http://dx.doi.org/10.1016/j.conbuildmat.2016.12.128
0950-0618/

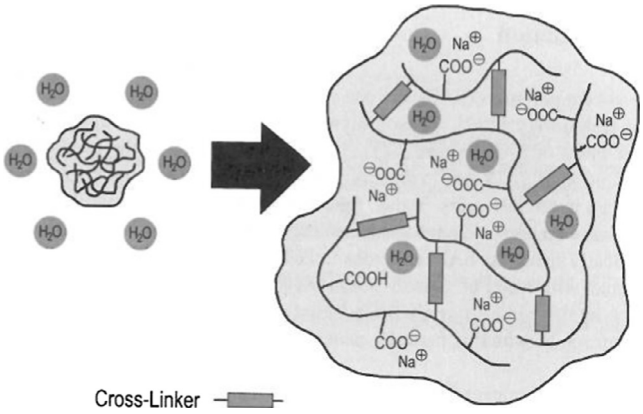

Fig. 1. SAP polymer network based on polyacrylic acid (courtesy of BASF) [7].

cement-based materials systems containing SAP and other cementitious materials as presented in Fig. 2 is therefore of interest in this study.

Fig. 2(a) is the initial condition which shows homogenous dispersion of cement particles, water, SAP and aggregates. Fig. 2(b) represent the state when SAP has reached final absorption and Fig. 2(c) refers to the state after desorption when the water has been transported into the cementitious matrix and almost empty pore remains [7].

The implication from Fig. 2 is that, as the cement hydration progresses, the space occupied by the swollen SAP particle after fluid absorption eventually form voids in the cured concrete. An evaluation of the influence of SAP contents and curing age on air voids sizes and distribution within the concrete is therefore important to the study of mechanical behaviour of HPC containing SAP.

SAP's effectiveness as IC-agent is dependent on its swelling ratio. This is defined as the rate at which SAP absorbs and releases water and the spacing within the SAP particles in concrete [10]. These factors are noted to be highly reliant on the structure and polymerisation technique of the SAP. The SAP particle size is also noted to influence the absorption of pore fluids. Jensen & Hansen [11] offered that very large SAP particles may have a reduced efficiency due to insufficient time for water uptake during mixing while very small SAP particles on the other hand, may also show reduced absorption as caused by less active surface zone compared to the bulk. Esteves [12] confirmed the significant influence of SAP particle size on both the amount of pore solution absorbed and the rate of water absorption.

Many research reports of SAP absorption of synthetic pore fluids exists with different absorption reported based on the method adopted and time of measurement. Jensen & Hansen [11] gave an absorption value of 20 g/g in 60 min for suspension-polymerised SAP (round particles of average 200 μm size), while a solution-polymerised SAP (crushed irregular particles of 125–250 μm size) was reported to absorb 37 g/g in 30 min. The SAP swelling in cement pastes gave a total absorption of about half the amount shown in the cement pore solution (CPS) which in turn is several times less than the absorption in distilled water [11].

Craeye & De Schutter [13], using SAP particles sizes of 100–800 μm, arrived at 130 g/g in distilled water after 5 min but above 500 g/g water absorption after 24 h. The latter absorption level was then used to estimate the SAP to be added to concrete in their study [13] with no account taken for the SAP's much less absorption in CPS than in water. Using an optical microscope, Esteves [12] observed the growth of individual SAP particles in the CPS over time. The work concludes that particle size had a significant influence on both the absorption kinetics and total amount of absorbed fluid.

SAP absorption in cement paste is more difficult to determine when compared to absorption in CPS. Determination of SAP absorption in CPS is generally by the use of the "tea-bag" test [14] or the "beaker test" [15] method with some disparity argued to exist in value obtained in comparison to the required additional water for SAP sorption in cement paste and concrete [11]. The distribution of the SAP particles in concrete is also an issue of concern, as the particles can form clusters or agglomerate [8]. Also noted in addition to issues raised above is the need to investigate crushing possibility of swollen SAP, especially the larger particles during vigorous mixing [7,12]. This postulation on crushing of SAP particles remained unverified till date based on available literature.

A popular approach adopted by researchers in estimating SAP absorption in cement pastes and concrete is by observing the changes in rheology of mixtures containing SAP. Slump flow was compared as a function of additional mixing time (up to 15 min) of concrete mixtures containing SAP in the works of Mönnig [8,16] to arrive at absorption of 10 ml/g and 45 ml/g for two SAP types. Most water uptake by the SAP was judged to occur in the first five minutes [16]. Dudziak & Mechtcherine [17] estimated SAP absorption in a coarse-grained fibre-reinforced UHPC by adjusting the water to obtain the same slump flow of a reference mixture. Rheological properties over time for cement-based mortar conducted using a rheometer was reported in [14] for data on yield stress and plastic viscosity. The result was used for determination of required dosage of SAP by weight of cement (b_{woc}) for specific additional water. The study revealed monomer chains and

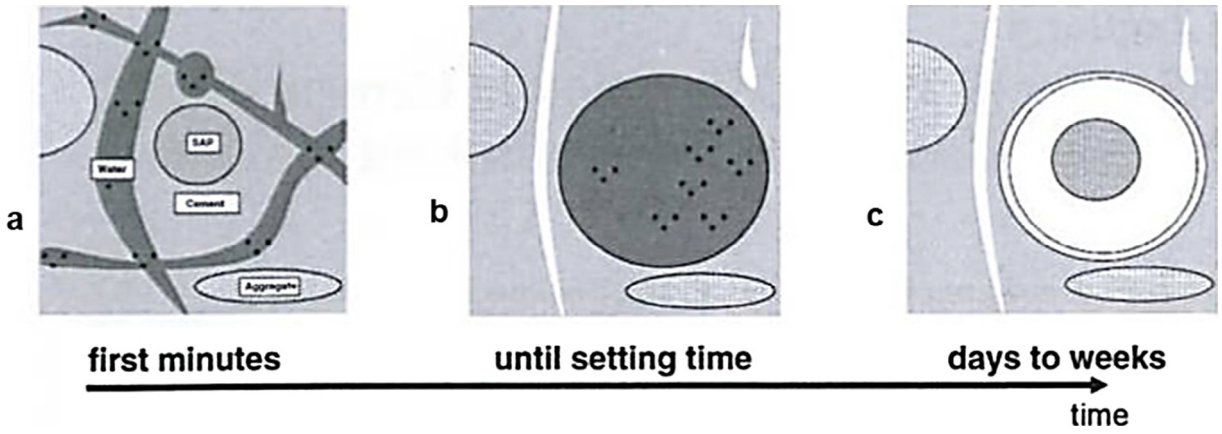

Fig. 2. Schematic representation of water migration in cement-based systems, after Mönnig [8].

polymerisation method of the specific SAP type, the particle size and the amount of free water available, all has direct influence on the absorption and desorption kinetics of SAP. Esteves [18] using optical microscope with the Fick's law arrived at SAP absorption of 13.2 ml/g in cementitious materials. A more recent study by Esteves [12] adopted and recommended Laser diffraction particle size analysis approach as the standard method for determination of absorption capacity of SAP for use in cement-based materials.

Approaches adopted by researchers for determination of SAP absorption capacity in cement pastes and concrete can be classified as follows:

(i) those based on the principle of stereology [19];
(ii) collection of digital images from polished paste surface using a high resolution scanner in combination with scanning electron microscopic (SEM) images for comparing particle size distribution of SAP at both the dry and swollen state at 2D image analysis level [17,20,21]; and
(iii) use of X-ray micro-tomography (3D images) for dry SAP particle size distribution and their distribution in high-performance mortars [22].

Laustsen et al. [23] and Maire & Withers [24] emphasised the need for proper characterisation of air voids in hardened concrete to include the knowledge of both size distribution and spatial distribution of the air voids. Characterisation of the air voids is noted to adopt linear-traverse method and the modified point-count method [25,26]. Both methods adopts 2D observations to describe 3D structures, hence the limitations of influence of results obtained by sample preparation and hence, inaccuracies in air void volumes determined. The use of X-ray computed tomography (CT-scanning) being a powerful measuring technique which provides information about the 3D structure of a sample without any prior preparation [27,28] thereby comes in handy for better air void analysis. Information on the influence of curing age and SAP contents on the air void distribution in concrete and cementitious materials are also of importance for a proper and appropriate use of SAP as IC-agent in concrete construction.

This paper reports on 3D volume analysis of the air voids in HPC containing SAP as IC-agent using commercial computer software having little operators influence as recommended by Laustsen et al. [23]. The concrete samples used for the image analysis were also made to appropriate sizes (50 mm Θ × 100 mm cylinders), the minimum size whole concrete (i.e. not a cut portion) in conformity with the standard's [29] requirement for the nominal aggregate size (13 mm) used for the HPC to give a true reflection of the actual pore and void states. Result of single specimen (stage I) analysis of this experiment was reported in an earlier publication [30] which recommended further studies on influence of SAP addition on the mechanical properties of very low W/B concrete containing other cementitious materials with examination of effect of curing age. This paper presents the result of Stage II (triplicate specimen) of the experiment on the air void analysis of the HPC containing SAP. It further examines the influence of hydration period; SAP size; SAP content and binder type on the air void size, sphericity and distribution.

2. Experimental investigation

2.1. Materials

Two sizes of SAP (<300 μm *with product label FLOSET CS 27 and* <600 μm labelled *FLOSET CC 31*) were used at different SAP contents: 0%, 0.2%, 0.3% and 0.4% by weight of binder. The SAP are thermoset polymers specifically covalently cross-linked polymers of acrylic acid and acrylamide, obtained from bulk solution polymerisation and neutralised by alkali hydroxide, which according to Schrofl et al. [2] have been proven efficient as internal curing agents in concrete. The SAP absorption capacity determined by tea-bag test is shown in previous work [31] to be 250 g/g in distilled water and 25 g/g (i.e. 2500 %) in cement pore solution (CPS) for both SAP grain sizes. The SAP particles were stored sealed as received in the plastic bags in a wooden cupboard to prevent exposure to moisture from the atmosphere until use.

A natural sand with minimum particle size of 300 μm (i.e. all the particles smaller than 300 μm was removed using a sieve) was used in compliance with requirement for fine aggregate specification for HPC production [32–34]. The sand has the following physical properties: Fineness Modulus (FM = 2.79), coefficient of uniformity (C_u = 2.43), coefficient of gradation (C_c = 1.02), dust content (0.3%) and is of medium sand classification [35] as observed in the sieve analysis reported in [36]. Crushed greywacke stone with nominal size of 13 mm was used as the coarse aggregate. CEM I 52.5N conforming to EN 197 [37] was the binder with silica fume, corex slag and fly ash added as cement extender while Premia 310 (a PCE) supplied by Chryso, was added as superplasticiser. The composition of the reference HPC mixtures is shown in Table 1.

Specimen designation for the various HPC mixtures as adopted in this study is presented in Table 2.

2.2. Methods

Four reference HPC mixtures of different binder combination types (cement, silica fume, fly ash and corex slag) and W/B (M_{1F} & M_{1S} (0.2); M_2 (0.25) and M_3 (0.3)) were adopted for the experiment. The 28-day characteristic strength (f_{ck}, cube) of 70 MPa minimum (i.e. C55/67 – C100/115 HSC) were made using the method described in Aïtcin [32] for HPC. Other HPC mixtures having varied SAP contents (0.2%; 0.3% and 0.4%) for the two SAP sizes (SP_1 – the smaller and SP_2) were then made for the respective HPC mixtures with extra water provided for SAP absorption on basis of 25 g/g arrived at from the tea-bag test. Consistency of the fresh HPC mixtures was determined using the slump flow table [38] and similar values observed for all the mixture irrespective of SAP content. The concrete was cast in 50 mm Θ × 100 mm cylindrical moulds and cured in water at 20 ± 3 °C for different hydration periods (i.e. 7, 28, 56 and 90 days respectively) in accordance to relevant BS Standards – [29,39–42]. The hardened HPC specimens were then placed in the oven at 40 °C for 30 min after removal from curing tank at respective hydration period to dry the specimen (i.e. to prevent occurrence of artefacts on the scanned images if moist concrete is subjected to CT scanning) before taken to the CT scanner for analysis. Mix M_{1F} and M_{1S} are both of the same W/B (0.2) but M_{1F} contains fly ash whereas M_{1S} has corex slag as supplementary cementitious material (SCM). The dry hardened HPC was subjected to X-ray CT scanning for the determination of the air void distribution. The 3D X-ray images were then examined and analysed using Avizo Fire, version 9.0 [43] and VG Studio Max 2.2 [44] to filter and classify the individual voids for determination of the sizes, distribution and volume analysis of void created by SAP in the HPC with the respective influence of binder type, water/binder, SAP content and curing age examined. The CT scanning was also used to affirm the grain sizes and distribution of the dry SAP particles.

The 3D X-ray images were obtained using a General Electric Phoenix VTomeX L240 X-ray micro computed tomography (micro-CT) scanner. Each concrete specimen was mounted in a less dense cardboard tube to reduce external influences on the samples during the scan. Reconstruction was performed with system supplied Datos Reconstruction software. The voxel size was set to 100 μm with settings at 170 kV and 150 μA for X-ray generation and image acquisition settings was 500 ms per image. The 3D

Table 1
Mix constituents of HPC mixtures.

Constituents	Reference mixes (kg/m^3)			
	M_{1F}	M_{1S}	M_2	M_3
Water	125	125	134	155
Cement (CEM I 52.5 N)	530	530	540	500
Coarse aggregate (13 mm nominal)	1050	1050	1050	1050
Sand (retained on 300 μm sieve)	590	590	710	700
Fly ash*	122.5	0	0	0
Corex slag*	0	122.5	0	0
Silica fume	52.5	52.5	40	40
Superplasticiser (Chryso Premia 310)	21	21	16	5.4
Water/binder ratio	0.2	0.2	0.25	0.3

* Fly ASH (FA) and Corex slag (CS) were used as additional alternative supplementary cementitious materials (SCM) incorporated at same proportion.

Table 2
Specimen designation of the HPC mixtures.

Specimen designation	Binder composition
	Binder Type 1 (binary cement) = OPC (92.5%) + (SF (7.5%)
M_2	Reference mixture for binder Type 1 (0.25 W/B)
M_2SP_1-0.2	M_2 + SAP size1 (0.2% b_{wob} content)
M_2SP_1-0.3	M_2 + SAP size 1 (0.3% b_{wob} content)
M_2SP_1-0.4	M_2 + SAP size 1 (0.4% b_{wob} content)
M_2SP_2-0.2	M_2 + SAP size 2 (0.2% b_{wob} content)
M_2SP_2-0.3	M_2 + SAP size 2 (0.3% b_{wob} content)
M_2SP_2-0.4	M_2 + SAP size 2 (0.4% b_{wob} content)
M_3	Reference mixture for binder Type 1 (0.30 W/B)
M_3SP_1-0.2	M_3 + SAP size 1 (0.2% b_{wob} content)
M_3SP_1-0.3	M_3 + SAP size 1 (0.3% b_{wob} content)
M_3SP_1-0.4	M_3 + SAP size 1 (0.4% b_{wob} content)
M_3SP_2-0.2	M_3 + SAP size 2 (0.2% b_{wob} content)
M_3SP_2-0.3	M_3 + SAP size 2 (0.3% b_{wob} content)
M_3SP_2-0.4	M_3 + SAP size 2 (0.4% b_{wob} content)
Ternary cements (0.20 W/B)	
M_{1F}	Reference mixture for binder Type 2 = OPC (75.0%) + SF (7.5%) + FA (17.5%)
$M_{1F}SP_1$-0.2	M_{1F} + SAP size 1 (0.2% b_{wob} content)
$M_{1F}SP_1$-0.3	M_{1F} + SAP size 1 (0.3% b_{wob} content)
$M_{1F}SP_1$-0.4	M_{1F} + SAP size 1 (0.4% b_{wob} content)
$M_{1F}SP_2$-0.2	M_{1F} + SAP size 2 (0.2% b_{wob} content)
$M_{1F}SP_2$-0.3	M_{1F} + SAP size 2 (0.3% b_{wob} content)
$M_{1F}SP_2$-0.4	M_{1F} + SAP size 2 (0.4% b_{wob} content)
M_{1S}	Reference mixture for binder Type 3 = OPC (75.0%) + SF (7.5%) + CS (17.5%)
$M_{1S}SP_1$-0.2	M_{1S} + SAP size 1 (0.2% b_{wob} content)
$M_{1S}Sp_1$-0.3	M_{1S} + SAP size 1 (0.3% b_{wob} content)
$M_{1S}SP_1$-0.4	M_{1S} + SAP size 1 (0.4% b_{wob} content)
$M_{1S}SP_2$-0.2	M_{1S} + SAP size 2 (0.2% b_{wob} content)
$M_{1S}SP_2$-0.3	M_{1S} + SAP size 2 (0.3% b_{wob} content)
$M_{1S}SP_2$-0.4	M_{1S} + SAP size 2 (0.4% b_{wob} content)

NB: The HPCs containing SAP had extra water provided on basis of 25 g/g SAP absorption determined by the tea-bag test.

image of HPC specimen is shown in Fig. 1a while Fig. 1b shows the 2D slice image of same.

The VGStudio Max 2.2 analysis require surface selection to identify and classify the colour-map/grey scale for voids analysis in the specimen with a defect analysis performed on these voids to determine the size and abundance of the void. The results from the analysis include size, abundance, sphericity and volume of the voids (see Fig. 3).

Image analysis using the Avizo Fire 9.0 involved various stages of image viewing, visualisation, and processing which can be automated and done with minimum human input. The workflow in the Avizo entails filtering, segmentation, analysis, surface generation, measurements and animation.

Details of the method adopted for the 3D volume analysis can be found in recent literatures [24,28]. The investigation of air voids in the concrete specimen via the CT scanning analysis involved two stages namely:

i. Single specimens analysis for the varied mixtures (has been reported in [30]) and
ii. Triplicate specimens analysis of three HPC mixtures (M_{1F}, M_2 and M_3) studied after 7 and 28 days curing in water. Triplicates of M_2 specimen were studied with both sizes of SAP (SP_1 and SP_2) – 42 concrete cylinders; while M_{1F} and M_3 triplicates were studied for SP_1 only – also 42 concrete cylinders.

This paper presents the result of the Stage II with some further discussion on the Stage I analysis.

The Stage II (triplicate specimen) analysis was conducted to verify reason for variation in the results reported in Stage I [30]. While casting the triplicate HPC specimens (Stage II), the fresh concrete were kept on the vibration table for longer time (10 min instead of the 5 min of Stage I) to further ensure that entrapped air voids in the mixtures are minimised.

Particle size distribution for the unhydrated SAP sample was carried out by scanning the two SAP grain sizes separately in a transparent cylindrical container. Reconstruction was performed as explained with system supplied Datos Reconstruction software and analysis conducted with the Avizo Fire following the steps stated previously. The scanning was done at 2 μm voxel size for the SAP particles actual size to be captured while a crop of 80 mm × 40 mm × 40 mm was made centrally from the VGI file when loaded before thresholding. Stage II analysis involved complete particle distribution of the dry SAP samples rather than individual particle examination as reported in [30]. Fig. 4a shows a 3D image of separated SAP particles with different colours depicting various size categories while Fig. 4b gives the 2D image of centrally cropped dry SAP specimen being analysed with the separated SAP particles in blue colour with spaces within.

3. Results and discussion

3.1. SAP sizes and morphology

The SAP particles were observed to be of varied sizes and shapes and they are mostly angular and irregular in shape and not totally spherical. The CT scanning (3D) image analysis (Fig. 5) revealed the SAP grain sizes to be in the range of 0 to 300 μm (SP_1) and 0 to 500 μm (SP_2). These agree well with the manufacturer's specification of ⩽300 μm (SP_1) and ⩽600 μm (SP_2). Table 3 shows the frequency distribution of the particles (using class intervals of 25 μm) while Fig. 6 presents the cumulative volume (%) present for the size classes in diameter. About 50% of the SP_1 particles were lower than 160 μm while 50% of SP_2 is below 260 μm.

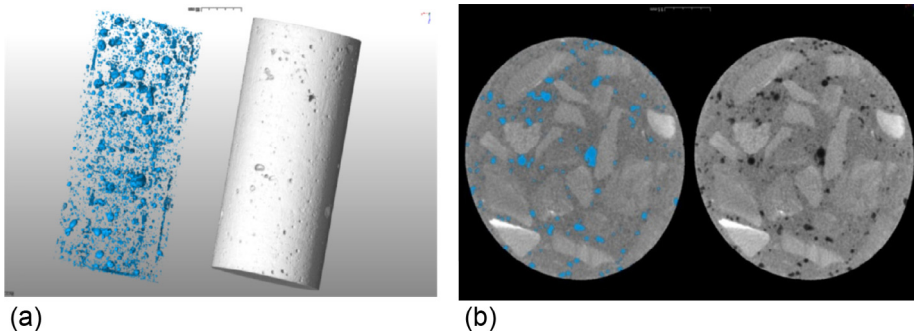

Fig. 3. 100 μm scan of HPC cylinder – (a) 3D visualisation and (b) thresholding applied to 2D image [28,30].

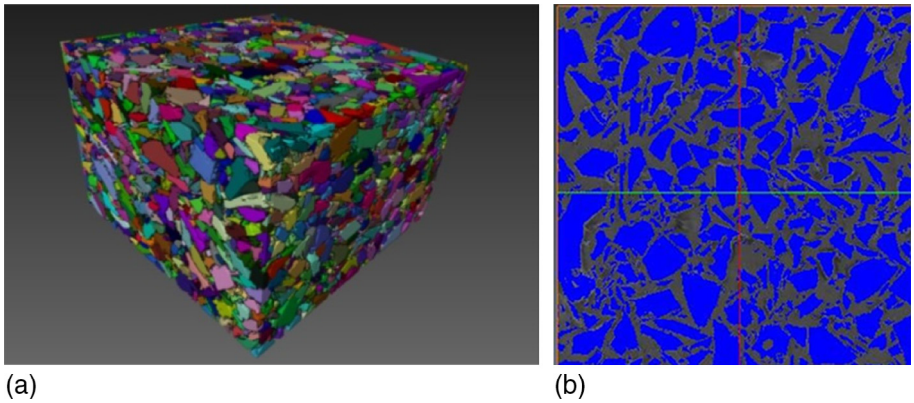

Fig. 4. 3D Image of separated dry SAP particles with colour indicating size classifications (a) and (b) centrally cropped CT image of dry SAP particles obtained from 3D VGI file.

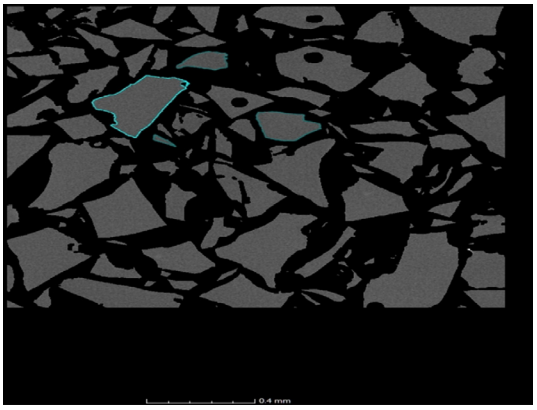

Fig. 5. CT image of examination of individual SAP particles obtained from a 3D VGI file [30].

Table 3
Frequency distribution of SAP particles.

Diameter	Volume	Frequency	
μm	mm^3	SP_1	SP_2
0–25	0.0000082	6587	22436
26–50	0.0000654	997	133
51–75	0.0002209	2437	594
76–100	0.0005236	1585	681
101–125	0.0010227	887	449
126–150	0.0017671	522	245
151–175	0.0028062	309	180
176–200	0.0041888	191	113
201–225	0.0059641	121	84
226–250	0.0081812	88	76
251–275	0.0108892	32	56
276–300	0.0141372	12	57
301–325	0.0179742	0	25
326–350	0.0224493	0	26
351–375	0.0276117	0	14
376–400	0.0335103	0	12
401–425	0.0401944	0	8
426–450	0.0477129	0	3
451–475	0.0561151	0	1
476–500	0.0654498	0	0

The study also determined the sphericity of the SAP particles. Sphericity is a measure of the roundness of a shape. A sphere is the most compact solid, so the more compact an object is, the more closely it resembles a sphere. Sphericity is a ratio and therefore a dimensionless number. Sphericity Φ_s is defined as:

$$\Phi_s = \frac{6V_p}{D_p A_p} \quad (1)$$

where V_p is the volume of the object, A_p is its surface area, and D_p is the diameter of a sphere with the same volume ($\pi D_p^3/6$).

A close observation of the SAP particles individually (Fig. 5) reveals that some particles have hollow voids (i.e. entrapped inclusions representing closed pores) within at the dry state. The entrapped inclusions can be argued to result from the production process of the SAP type used in this study. This according to [46] involves having aqueous monomer solution of certain concentration (25–40%) cooled down to 0–10 °C and transferred to a reactor, made of an endless belt. The monomer solution poured in and polymerisation running adiabatically forms a rubber like gel which is then cut by an extruder into smaller pieces and dried. The resulting SAP from this type of polymerisation process is known to give irregular shapes as observed for the SAP used in this study (Fig. 5).

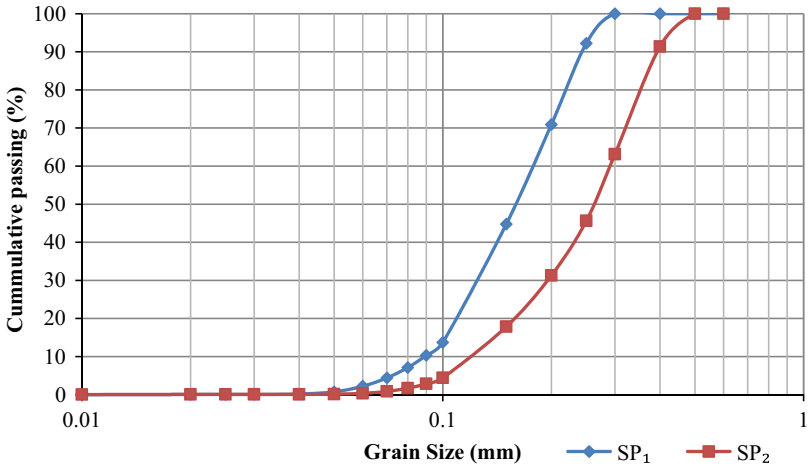

Fig. 6. % cumulative volume present of various particle sizes for SP_1 and SP_2.

Sphericity assessment of the particles shows the SAP particles has average sphericity values of 0.86 (SP_1) and 1.14 (SP_2), hence the larger the SAP size, the less spherical it becomes. The maximum and minimum sphericity values are 1.61 and 0.61 (SP_1); 1.61 and 0.32 (SP_2) respectively. The upper limit value of 1.61 being above 1.0 expected for a perfect sphere is a confirmation of presence of empty hollow spaces within some SAP particles The particles having hollow voids within were noted to give sphericity values above 1.0, thereby making average sphericity values not to be a good measure of how spherical the SAP particles are.

The SAP air voids created in concrete on basis of 25 g/g SAP absorption (i.e. swollen SAP) in CPS calculated with an assumption of sphere shape for SAP gave a value of three multiple of the dry SAP size (i.e. size range of 75 μm–900 μm class intervals for SP_1 (swollen SAP)) and (75 μm–1500 μm class intervals for SP_2 (swollen SAP)) taking clue from Laustsen et al. [23]. This gave a clearer, detailed and more reliable assessment than the approach adopted in the Stage I study [30] which was only random examination of individual SAP particle and gave a resultant size range of dry SAP as 75 μm–350 μm and the swollen SAP size as 225 μm–1050 μm.

3.2. 3D void analysis of HPC specimens

The CT scanning analysis enhanced an in-depth view of the internal structure of the HPCs with the objective of examining the pore spaces within the cement paste matrix and a classification of the air voids created by the swollen SAP after desorption of the absorbed water. Fig. 7 presents a snap shot of the centrally cropped (filtered and segmented) HPC specimen with air voids in blue colour within the cement paste matrix. The observed air voids were well distributed and of varying sizes and shapes.

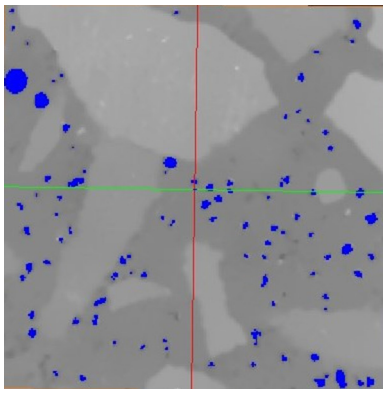

Fig. 7. Centrally cropped (filtered and segmented) HPC with air voids in blue colour. (For interpretation of the references to colour in this figure legend, the reader is referred to the web version of this article.)

Note that the discussion in the following sections on air voids adopts the use of the following terms: SAP voids, SAP range voids and large voids. *SAP voids* refer to the air voids created by SAP in the HPCs. Hence for SP_1, the air voids sizes of 0–900 μm diameter applies while the void sizes of 0–1500 μm diameter is implied for SP_2. The reference mixtures do not have SAP included and hence has no SAP voids. *SAP range voids* refers generally to all air voids present in the HPC within the SAP voids sizes (i.e. 0–1500 μm) for all HPCs. *Large voids* on the other hand refers to air voids >1500 μm in diameter.

3.3. Influence of SAP contents on air void distribution

Result of the single specimen analysis presented in [30] reported increased SAP voids and total voids % as SAP contents and W/B increased with some anomalies. Some excess air was believed to be trapped within the concrete hence creating large air voids which are not SAP created voids. These large air voids form part of what was used to calculate the total void % but were excluded in the calculation of SAP voids % and SAP range voids %. High numbers of air voids larger than SAP voids (>900 μm for SP_1 and >1500 μm for SP_2) were also reported with arbitrary extremes of very small and large air voids volumes. These contributed to the value obtained for total porosity as calculated from the X-ray CT scanning analysis. Result of the triplicate samples as presented in the current study give a better conclusion on the influence of SAP contents and W/B or mixture type on the air void distribution of HPC.

SAP range void % for the single specimen analysis were generally about half the value of the expected porosity using the 25 g/g SAP absorption capacity determined via the tea-bag test, while the demoulded density gave similar but slightly higher values as the calculated expected porosity. Total porosity obtained from the CT scanning analysis was observed to be lower in value to the de-moulded density [30]. This implies that porosity on the scale investigated in the HPC generally decreased with cement hydration over time. An indication that the initial SAP created voids in fresh concrete reduces in size and hence volume with increased concrete age. Cement hydration product is believed to occupy the air spaces created by the swollen SAP which agrees

with the report of a previous study by Justs et al. [45]. It was observed [45] that the swollen SAP cavities in cement pastes were partially filled with portlandite during cement hydration. Further hydration at longer ages is thereby expected to reduce the size of SAP created voids and hence a reduction in air voids of the HPC with SAP as hydration progresses with age.

It can be deduced therefore that the extra water added to the mixing water for SAP absorption in concrete mixtures should be maintained at 12.5 g/g (i.e. halve the 25 g/g used in this study), This sorption level holds true for the SAP type (covalently cross-linked polymers of acrylic acid and acrylamide obtained from bulk solution polymerisation and neutralised by alkali hydroxide) used in this study. This agrees well with findings of previous studies [47], [48] for its effectiveness as IC-agent. This is the optimum water required for effective internal curing in the HPC and adherence to this will reduce occurrence of the SAP's created air voids and hence avert the strength reduction effect of the SAP addition observed.

Fig. 8 (plotted from results earlier presented in [30]) shows that for the single specimen analysis, the SAP voids (SP_1 (0–900 μm); SP_2 (0–1500 μm)) increased with increase in SAP contents for all HPC mixtures irrespective of the SAP size. The higher the binder (i.e. fines) contents also, the lower the porosity. The SAP range voids % was also reported in [30] to decrease as the hydration period increased with some anomalies while increase in SAP size and contents resulted in increased SAP range voids % for all hydration periods [30]. The values reported in Fig. 8 were obtained from the histogram plot of void volume/diameter and frequency of occurrence for the single specimen. These values are exact for the respective specimen, hence no further statistical interpretation possible.

The Stage II (triplicate specimen) analysis conducted to verify reason for variation in the results reported in Stage I further affirm that SAP voids, SAP range voids and total voids percentages increased as the SAP size and contents increases.

Table 4 shows summary of the voids distribution in triplicate for M_2 – HPC mixtures with both SAP types. The standard deviation[1,2,3] calculated for the SAP voids %, total porosity % and SAP range voids % respectively as shown in Table 4 reveals the values are generally concentrated around the mean values reported for all the specimens. The standard deviation[1] for SAP voids % falls within 0 and 0.39 for both SP_1 and SP_2 specimens. The standard deviation[2] for total porosity is in the range 0.08 to 0.52 for both SP_1 and SP_2 specimen while standard deviation[3] for SAP range voids % lies within 0.07–0.49.

The use of triplicate HPC specimen reveals no variation in the trend of the progressive increase of SAP range voids % and total porosity % in the HPC as the SAP size and contents increase. The SAP range void % (i.e. <1500 μm as defined in Section 3.2) clearly decreased as curing age increases with no ambiguity using the triplicate samples (Fig. 9). The maximum void sizes in the Stage II analysis were also observed to be within similar value range (20–60 mm^3) for both SAP sizes (Table 4).

The total air void % in the mixtures and average void diameters were noted to be lower than the earlier values obtained for single specimen analyses [30]. The longer time of vibration (10 min) of the HPCs as against the 5 min used for Stage I during concrete casting can therefore be seen to result in better compaction and reduction of trapped air voids within the concrete. The number of large voids (>1500 μm) is observed to be of a uniform range (25 for reference and SP_1 mixtures and 29–46 for SP_2) at 7 days of hydration and at 28 days of hydration (15–30 for both SAP sizes) for M_2 – HPC mixtures. The average pore diameter determined (taking the voids as sphere) were seen to be more uniform for both SAP sizes and at both hydration periods (0.5–0.6 mm) in the triplicate specimen analyses. The number of large voids, SAP porosity and total porosity decreased as the curing age increases for both SAP sizes in triplicate specimen analysis of M_2 – HPC mixtures.

Fig. 9 shows a plot of the SAP range voids % against the curing age for Stage II analysis of the M_2 – HPC mixture.

3.4. Influence of W/B, binder type and curing age on air void distribution

The Stage II analysis using triplicate specimen with SP_1 is as presented in Table 5 showing summary of influence of curing age and W/B on air void distribution for three HPC mixtures (M_{1F}, M_2 and M_3), while influence of curing age and SAP sizes for M_2 – HPC mixtures is as earlier presented in Table 4. The standard deviation[1,2,3] ($SD^{1,2,3}$) for the SAP void %, total porosity % and SAP range voids % respectively for the various mix composition, W/B and the curing ages shown in Table 5 affirms that the values obtained for the triplicate specimen analysis are concentrated around the mean values reported in all cases. The SAP voids % for $M_{1F}SP_1$-0.4 was noted to have the widest spread (an SD^1 value of 0.54) from the mean value reported. Similar trend is observed for total porosity % and SAP range voids % with same specimen $M_{1F}SP_1$-0.4 having the highest $SD^{2,3}$ values of 0.65 for both.

Fig. 10 further shows a plot of SAP range voids % (i.e. all voids below 1500 μm diameter size as defined in Section 3.2) against the curing ages examined (7 and 28 days) for the triplicate samples of M_3 and M_{1F} HPC series.

The result shows that in the triplicate specimens' analyses, the SAP voids % and total voids % increases as the SAP contents increases while SAP range voids % decreased as the curing age increases for all the HPC mixtures studied. The reference HPC with 0.25 W/B (M_2 – binary cement binder) has the lowest porosity values followed by M_{1F} – ternary cement (0.2 W/B with fly ash), while M_3 – binary cement (0.3 W/B) has the highest porosity value.

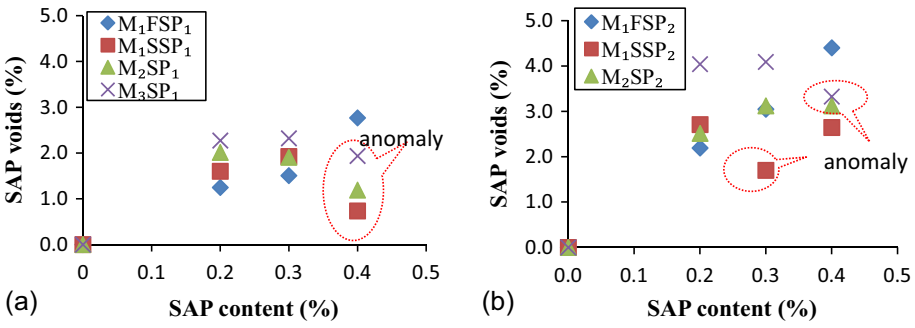

Fig. 8. SAP voids % against SAP content % (a) SP_1; (b) SP_2.

Table 4
Summary of void distribution in triplicate HPC-M_2 with both SAP types.

Curing age influence	Ref	SAP1			SAP2		
M_2-7 Day Series	M_2	M_2SP_1-0.2	M_2SP_1-0.3	M_2SP_1-0.4	M_2SP_2-0.2	M_2SP_2-0.3	M_2SP_2-0.4
SAP pore expected[+]	0	3.4	5.01	6.56	3.4	5.01	6.56
No of voids 1500 μm	25	25	25	25	29	36	46
SAP voids %	0.00	0.95	1.16	1.30	1.00	1.71	1.91
Standard deviation[1]	0.00	0.39	0.23	0.19	0.24	0.24	0.27
Total Porosity[++] %	0.81	1.42	1.68	1.84	1.27	2.04	2.32
Standard deviation[2]	0.11	0.47	0.29	0.28	0.38	0.35	0.46
SAP range voids %	0.58	1.19	1.42	1.60	1.00	1.71	1.91
Standard deviation[3]	0.16	0.42	0.26	0.27	0.24	0.24	0.27
Max. void size (mm^3)	23.716	35.789	17.927	34.185	21.598	34.045	50.996
Av. void diameter (mm)	0.658	0.501	0.470	0.457	0.616	0.570	0.594
M_2-28 Day Series	M_2	M_2SP_1-0.2	M_2SP_1-0.3	M_2SP_1-0.4	M_2SP_2-0.2	M_2SP_2-0.3	M_2SP_2-0.4
No of voids >1500 μm	18	16	23	22	14	36	30
SAP voids %	0.00	0.60	1.02	1.20	0.90	1.19	1.46
Standard deviation[1]	0.00	0.15	0.32	0.32	0.22	0.34	0.24
Total Porosity %	0.72	0.94	1.47	1.74	1.04	1.53	1.74
Standard deviation[2]	0.08	0.15	0.41	0.51	0.20	0.52	0.35
SAP range voids %	0.55	0.79	1.25	1.52	0.90	1.19	1.46
Standard deviation[3]	0.07	0.13	0.39	0.49	0.22	0.34	0.24
Max. void size (mm^3)	25.260	42.208	56.197	60.147	21.837	38.206	18.764
Av. void diameter (mm)	0.542	0.525	0.429	0.464	0.549	0.576	0.550

Standard deviation[1, 2, 3] refers to the standard deviation for SAP voids, Total Porosity and SAP range voids respectively in for the triplicate sample analysis.
[+] Expected pore content by volume based on the 25 g/g pore absorption used for provision of additional water calculated taking the swollen SAP as a spherical substance.
[++] Porosity calculated volumetrically using De-moulded density in comparison to designed density

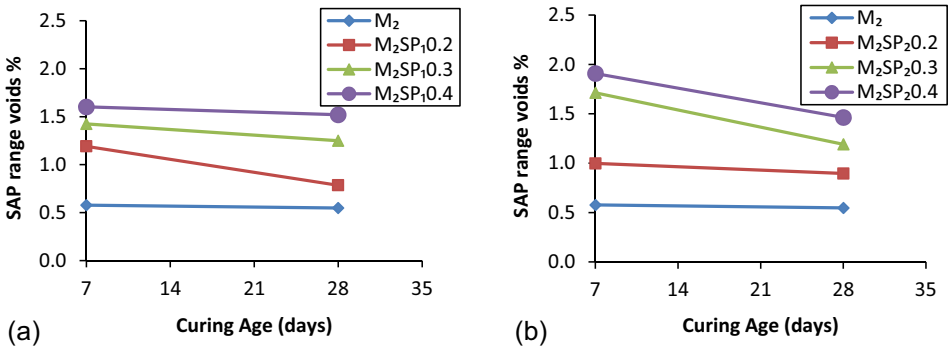

Fig. 9. SAP range voids % vs curing age for triplicate M_2 – HPCs (a) SP_1; (b) SP_2.

The maximum void size in the triplicate specimen analyses were seen to be of similar range of value (20–75 mm^3) for the HPC mixtures studied with only one variation observed in M_3. The average pore size (0.40–0.65 mm, in diameter) determined taking the void volumes as sphere was consistent for all HPC mixtures studied. There were no excessively large void present nor were there variations in the number of large voids (i.e. >1500 μm) for the three HPC mixtures examined for Stage II analysis.

It can therefore be inferred from this study that for very low W/B mixes SAP addition made additional internal water available for longer period of cement hydration leading to possible increase in structure of the cement hydration products and hence reduction in the voids present. This study revealed that the 25 g/g SAP absorption capacity result of the tea-bag test over-estimates the actual amount of water used up by SAP in the internal curing of HPC considering the fact that the solid constituents of the concrete were not incorporated in the tea-bag test SAP absorption simulation. The revelation from the 3D volume analysis of the HPC via CT scanning shows that SAP voids in the HPC is only about half (i.e. 12.5 g/g) of the tea-bag test provision of 25 g/g and this affirms that the required additional water for effective internal curing of the low W/B HPC by this SAP type is 12.5 g/g. The excess water of 12.5 g/g above the required is the observed SAP created voids and possibly the reason for the loss in compressive strength as observed in previous studies [26,45], [48].

Further works on ascertaining effect of this SAP type on cement hydration in HPC and the final products of hydration should offer good explanation to this development.

4. Conclusion and recommendation

Influence of SAP addition and curing age on the air voids distribution in HPC have been examined using a 3D volume analysis done through a micro-CT scanner for HPC mixtures of different W/B, binder types and SAP sizes. Also studied with the micro-CT scanner are the dry SAP particles size distribution, shape and sphericity. The result reveals that:

i. SAP particles studied are of varied sizes, mostly angular and irregular in shape and not spherical. The dry SAP particle size distribution analysed using micro-CT scanner (SP_1 – 0/300 μm; SP_2 – 0/500 μm) agrees with the manufacturer's specification (SP_1 < 300 μm; SP_2 < 600 μm).

Table 5
Summary of curing age influence and W/B on void distribution using triplicate specimens.

Curing age influence	7 Days				28 Days			
M_{1F}-Series	M_{1F}	$M_{1F}SP_1$-0.2	$M_{1F}SP_1$-0.3	$M_{1F}SP_1$-0.4	M_{1F}	$M_{1F}SP_1$-0.2	$M_{1F}SP_1$-0.3	$M_{1F}SP_1$-0.4
No of voids >1500 μm	32	26	30	23	16	39	31	32
SAP void %	0.00	1.08	1.43	1.54	0.00	0.68	0.85	1.07
Standard deviation[1]	0.00	0.09	0.35	0.54	0.00	0.14	0.21	0.32
Total Porosity %	1.39	1.58	2.09	2.10	1.20	1.40	1.41	1.68
Standard deviation[2]	0.08	0.14	0.52	0.65	0.40	0.20	0.13	0.41
SAP range voids %	1.09	1.33	1.80	1.88	1.06	1.03	1.12	1.38
Standard deviation[3]	0.01	0.11	0.42	0.65	0.37	0.15	0.18	0.40
Max. void size (mm^3)	75.487	31.194	55.396	27.652	26.329	42.09	29.902	35.399
Av void diameter (mm)	0.525	0.388	0.460	0.424	0.394	0.633	0.515	0.501
M_2-Series	M_2	M_2SP_1-0.2	M_2SP_1-0.3	M_2SP_1-0.4	M_2	M_2SP_1-0.2	M_2SP_1-0.3	M_2SP_1-0.4
No of voids >1500 μm	25	25	25	25	18	16	23	22
SAP void %	0.00	0.95	1.16	1.30	0.00	0.60	1.02	1.20
Standard deviation[1]	0.00	0.39	0.23	0.19	0.00	0.15	0.32	0.32
Total Porosity %	0.81	1.42	1.68	1.84	0.72	0.94	1.47	1.74
Standard deviation[2]	0.11	0.47	0.29	0.28	0.08	0.15	0.41	0.51
SAP range voids %	0.58	1.19	1.42	1.60	0.55	0.79	1.25	1.52
Standard deviation[3]	0.16	0.42	0.26	0.27	0.07	0.13	0.39	0.49
Max. void size (mm^3)	23.716	35.789	17.927	34.185	25.260	42.208	56.197	60.147
Av. void diameter (mm)	0.658	0.501	0.470	0.457	0.542	0.525	0.429	0.464
M_3-Series	M_3	M_3SP_1-0.2	M_3SP_1-0.3	M_3SP_1-0.4	M_3	M_3SP_1-0.2	M_3SP_1-0.3	M_3SP_1-0.4
No of voids >1500 μm	36	35	26	21	18	12	27	26
SAP void %	0.00	0.82	0.85	1.03	0.00	0.66	0.72	0.79
Standard deviation[1]	0.00	0.16	0.10	0.20	0.00	0.35	0.19	0.15
Total Porosity %	1.67	1.60	1.48	1.53	0.84	0.99	1.28	1.38
Standard deviation[2]	0.08	0.63	0.15	0.24	0.32	0.53	0.29	0.26
SAP range voids %	1.34	1.28	1.23	1.34	0.67	0.88	1.02	1.14
Standard deviation[3]	0.01	0.42	0.16	0.22	0.26	0.48	0.25	0.22
Max. void size (mm^3)	61.863	18.602	29.805	57.332	21.941	22.042	55.997	32.302
Av void diameter (mm)	0.451	0.528	0.502	0.494	0.544	0.510	0.608	0.536

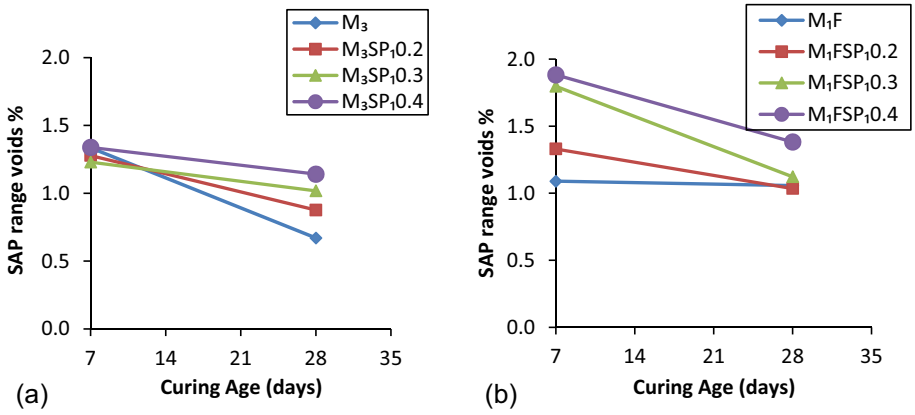

Fig. 10. SAP range voids vs curing age (triplicates specimen) for (a) M_3 (b) M_{1F}.

ii. All the HPC mixtures had micro-air voids present irrespective of SAP contents. SAP created voids are however more and follows same pattern as the distribution of the dry SAP particles.
iii. An increase in SAP content and also the W/B of the HPCs led to increase in SAP voids (<900 μm (SP_1); <1500 μm (SP_2) as defined in Section 3.2) and the total air voids.
iv. SAP addition to the limit of 0.3% b_{wob} enhanced a wider distribution of air voids in HPC and has little influence on the porosity of concrete for low W/B HPC.
v. The porosity created by SAP in the HPC were generally about half the porosity calculated expected value using the 25 g/g SAP absorption capacity determined via the tea-bag test. An indication that the initial SAP created voids in fresh concrete reduces in size and hence volume with increased concrete age as cement hydration products occupied the air spaces created by the swollen SAP confirming the findings of Justs et al. [45]. It follows that maintaining the water added to the mixing water for SAP absorption in concrete mixtures at 12.5 g/g (i.e. halve the 25 g/g used in this study), similar value to that suggested in previous studies [46,12] for this SAP type, will reduce occurrence of SAP created air voids in these HPCs and hence avert the strength reduction effect of SAP addition observed.

It can however be concluded that though SAP addition increase the air voids content in HPC, the influence will be minimal when the additional water for SAP absorption is maintained within 12.5 g/g (i.e. half the 25 g/g obtained in the teabag test).

Further studies on influence of this SAP type addition on the mechanical properties of very low W/B concrete (i.e. HPC)

containing other cementitious materials and a SEM/EDX analysis to ascertaining its effect on cement hydration in HPC and constituent final products of hydration are thereby recommended. This will further compliment results of studies carried in [45] out on cement pastes.

Acknowledgements

We acknowledge the following: Mr. Guillaume Jeanson (Construction Product Manager) SNF Floerger – ZAC de Milieux, 42163 ANDREZIEUX Cedex – FRANCE; Davy Penhard, FEI Visualisation Science Group; Dr. Anton du Plessis and Stephan le Roux, CT Scanner Unit, Central Analytical Facilities (CAF), Stellenbosch University, South Africa for the assistance received in materials procurement, use of facilities, softwares and time input in the analysis.

References

[1] ACI THPC/TAC, ACI Defines High Performance Concrete – the Technical Activities Committee Report (Chairman – H.G. Russell), 1999 www.concrete.org.
[2] C. Schröfl, V. Mechtcherine, M. Gorges, Relation between the molecular structure and the efficiency of superabsorbent polymers (SAP) as concrete admixtures to mitigate autogenous shrinkage, Cem. Concr. Res. 42 (6) (2012) 865–873.
[3] T.C. Powers, L.E. Copeland, H. Mann, Capillary continuity or discontinuity in cement pastes. Capillary continuity or discontinuity in cement pastes, Bulleting 110 (1959) 11–12.
[4] ACI (308-213) R13: "Report on internally cured concrete using pre-wetted absorptive lightweight aggregate", www.concrete.org.
[5] O.M. Jensen, P. Lura, Techniques and materials for internal water curing of concrete, Mater. Struct. 39 (9) (2006) 817–825.
[6] K. Kolver, O. Jensen (Eds.), Internal curing of concrete. State-of-the-art report of the RILEM technical committee 196-ICC, RILEM Report, 41, 2007, ISBN 978-2-35158-082-0, e-ISBN 978-2-35158-082-0.
[7] V. Mechtcherine, H.W. Reinhardt (Eds.), Application of superabsorbent polymers in concrete construction. State-of-the-art report of the RILEM TC 225-SAP, Springer, Heidelberg/Germany, 2012, ISBN 978-94-007-2732-8.
[8] S. Mönnig, Superabsorbing additions in concrete – applications, modelling and comparison of different internal water sources (Ph.D. thesis), University of Stuttgart, 2009, 164 pp.
[9] O.M. Jensen, P.F. Hansen, Water-entrained cement-based materials I: experimental observations, Cem. Concr. Res. 31 (4) (2001) 647–654.
[10] J. Siramanont, W. Vichit-Vadaka, W. Siriwatwechakul, The impact of SAP structure on the effectiveness of IC, in: International RILEM Conference on use of Superabsorbent Polymers and Other New Additives in Concrete, Technical University Denmark, Lyngby, Denmark, Proceeding Pro074, (15–18 August), 2010, pp. 243–252.
[11] O.M. Jensen, P.F. Hansen, Water-entrained cement-based materials II: experimental observations, Cem. Concr. Res. 32 (6) (2002) 973–978.
[12] L.P. Esteves, Recommended method for measurement of absorbency of superabsorbent polymers in cement-based materials, Mater. Struct. 48 (8) (2015) 2397–2401.
[13] B. Craeye, M. Geirnaert, G.D. Schutter, Super absorbing polymers as an internal curing agent for mitigation of early-age cracking of high-performance concrete bridge decks, Constr. Build. Mater. 25 (1) (2011) 1–13.
[14] V. Mechtcherine, E. Secrieru, C. Schröfl, Effect of superabsorbent polymers (SAPs) on rheological properties of fresh cement-based mortars – development of yield stress and plastic viscosity over time, Cem. Concr. Res. 67 (2015) 52–65.
[15] D. Yiamsawas, W. Kangwansupamonkon, O. Chailapakul, S. Kaitkamjornwong, Synthesis and swelling properties of poly[acrilamide-co-(crotonic acid)] superabsorbents, React. Funct. Polym. 67 (2007) 865–882.
[16] S. Mönnig, Water saturated super-absorbent polymers used in high strength concrete, Otto-Graf-J. 16 (2005) 193–202.
[17] L. Dudziak, V. Mechtcherine: Mitigation of volume changes of ultra-high performance concrete (UHPC) by using super absorbent polymers, in: E. Fehling et al. (Eds.), Proceedings of 2nd International Symposium on Ultra High Performance Concrete, Kassel University Press GmbH, 2008, pp. 425–432.
[18] L.P. Esteves, Superabsorbent polymers: on their interaction with water and pore fluid, Cem. Concr. Compos. 33 (7) (2011) 717–724.
[19] O.M. Jensen, Use of superabsorbent polymers in construction materials, in: 1st International Conference on Microstructure Related Durability of Cementitious Composites", October 2008, 13–15, Nanjing, Peoples Republic of China.
[20] V. Mechtcherine L. Dudziak, J. Schulze, H. Staehr, Internal Curing by super absorbent polymers (SAP) – effects on material properties of self-compacting fibre-reinforced high performance concrete, in: International RILEM Conference on Volume Changes of Hardening Concrete: Testing and Mitigation, Technical University of Denmark, Lyngby, Denmark., Proceeding Pro052 (20–23 August), 2006, pp. 87–96.
[21] V. Mechtcherine, L. Dudziak, S. Hempel, Mitigating early age shrinkage of Ultra-high performance concrete by using super absorbent polymers (SAP), in: T. Tanabe et al. (Eds.), Creep, Shrinkage and Durability Mechanics of Concrete and Concrete Structures – CONCREEP-8, Taylor & Francis Group, London, 2009, pp. 843–853.
[22] P. Lura, F. Durand, A. Loukili, K. Kovler, O.M. Jensen, Strength of cement pastes and mortars with superabsorbent polymers, in: International RILEM Conference on Volume Changes of Hardening Concrete: Testing and Mitigation, RILEM Proceedings PRO 52, RILEM Publications S.A.R.L., 2006, pp. 117–126.
[23] S. Laustsen, D.P. Bents, M.T. Hasholt, O.M. Jensen, CT measurement of small voids in concrete, in: O.M. Jensen, M.T. Hasholt, S. Laustsen (Eds.), Use of Superabsorbent Polymers and Other New Additives in Concrete, PR074, RILEM Publications, Technical University of Denmark, Lyngby, Denmark, 2010, pp. 153–162.
[24] E. Maire, P.J. Withers, Quantitative X-ray tomography, Int. Mater. Rev. 59 (1) (2014) 1–43, http://dx.doi.org/10.1179/1743280413Y.0000000023.
[25] EN 480-11, Admixtures for concrete, mortar and grout – test methods for determination of air-voids characteristics in hardened concrete, BSI, London.
[26] ASTM C457-10a, Standard test method for microscopical determination of parameters of the air-void systems in hardened concrete, U.S.A. www.astm.org.
[27] D.P. Bentz, P.M. Halleck, A.S. Grader, J.W. Roberts, Four-dimensional X-ray microtomography study of water movement during internal curing, in: O.M. Jensen, P. Lura, K. Kovler (Eds.), Volume Changes of Hardening Concrete: Testing and Mitigation, PR052, RILEM Publications, Technical University of Denmark, Lyngby, Denmark, 2006, pp. 11–20.
[28] A. Du Plessis, B.J. Olawuyi, W.P. Boshoff, S. Le Roux, Simple and fast method for 3D porosity analysis of concrete samples using X-ray computed tomography, Mater. Struct. 49 (1) (2016) 553–562.
[29] EN 12390-2, Testing of hardened concrete - making and curing specimen for strength tests, BSI, London, 2000.
[30] B.J. Olawuyi, W.P. Boshoff, 3D void analysis of high performance concrete containing superabsorbent polymers (SAP), in: International RILEM Conference on Application of Superabsorbent Polymers and Other New Admixtures in Concrete Construction, Technische Universitat Dresden, Dresden, Germany, PRO 95, 2014, pp. 81–91.
[31] B.J. Olawuyi, W.P. Boshoff, Compressive strength of high-performance concrete with absorption capacity of super-absorbing-polymers (SAP), in: Research and Applications in Structural Engineering, Mechanics and Computation – Zingoni (Ed.) © 2013 Taylor & Francis Group, London, 2013, pp 1679–1683, ISBN 978-1-138-00061-2.
[32] P.C. Aïtcin, High-Performance Concrete, Taylor & Francis, 1998.
[33] H. Beushausen, F. Dehn, High-performance concrete, in: G. Owens (Ed.), Fulton's Concrete Technology, 9th ed., Cement and Concrete Institute, Midrand, South Africa, 2009, pp. 297–304.
[34] A.M. Neville, Properties of Concrete, 5th ed., Pearson Educational Limited, England, 2012.
[35] M.S. Shetty, Concrete Technology – Theory and Practice, S. Chand and Company Limited, New Delhi, India, 2004.
[36] B.J. Olawuyi, W.P. Boshoff, Influence of particle size distribution on compressive strength and elastic modulus of high performance concrete, in: International Conference on Advances in Cement and Concrete Technology in Africa (ACCTA), Johannesburg, South Africa, 2013, pp 825–833.
[37] EN 197-1, Cement – composition, specifications and conformity criteria for common cements, BSI, London, 2000.
[38] INCAR, Summary of concrete workability test methods – Research Report – INCAR – 105–1, International Center for Aggregates Research (INCAR), Jan. 5, 2003.
[39] EN 12350-1, Testing of fresh concrete – Sampling, BSI, London, 2000.
[40] EN 12350-5, Testing of fresh concrete - Flow Table Test, BSI, London, 2000.
[41] EN 12390-1, Testing of hardened concrete – shape, dimension and other requirement for specimens and mould, BSI, London, 2000.
[42] EN 1992-1-1, Eurocode 2 – Design of concrete structures – General rules and rules for buildings, BSI, London, 1992.
[43] FEI Visualisation Science Group, Avizo Fire (version 9.0) – 3D Analysis software for Scientific and Industrials Data, 2013 www.vsg3d.com.
[44] Volume Graphics, VGStudio Max 2.2 – Application software for analysis and visualisation of industrial computed tomography/voxel data", 2013 www.volumegraphics.com.
[45] J. Justs, M. Wyrzykowski, D. Bajare, P. Lura, Internal curing by superabsorbent polymers in ultra-high performance concrete, Cem. Concr. Res. 76 (2015) 82–90.
[46] M.T. Hasholt, O.M. Jensen, K. Kolver, S. Zhutovsky, Can superabsorbent polymers mitigate autogenous shrinkage of internally cured concrete without compromising the strength?, Constr Build. Mater. 31 (2012) 226–230.
[47] M.T. Hasholt, M.H.S. Jespersen, O.M. Jensen, Mechanical properties of concrete with SAP – part I: development of compressive strength, in: O.M. Jensen, M.T. Hasholt, S. Laustsen (Eds.), Use of Superabsorbent Polymers and Other New Additives in Concrete, PR074, RILEM Publications, Technical University of Denmark, Lyngby, Denmark, 2010, pp. 117–126.